

UNFOLDING POLYNOMIAL MAPS AT INFINITY

WALTER D. NEUMANN AND PAUL NORBURY

1. INTRODUCTION

Let $f: \mathbb{C}^n \rightarrow \mathbb{C}$ be a polynomial map. The polynomial describes a family of complex affine hypersurfaces $f^{-1}(c)$, $c \in \mathbb{C}$. The family is locally trivial, so the hypersurfaces have constant topology, except at finitely many *irregular* fibers $f^{-1}(c)$ whose topology may differ from the generic or *regular* fiber of f .

We would like to give a full description of the topology of this family in terms of easily computable data. This paper describes some progress.

We will restrict mostly to the case that f has only isolated singularities. We show that the data then needed are local monodromy maps obtained by transporting a fixed generic fiber F around the irregular fibers, and the “Milnor fibers” of the singular points and singularities at infinity of f : these are certain submanifolds of F that describe the loss of topology at irregular fibers.

It is convenient to subdivide this necessary data as follows. For each irregular fiber we need

- the Milnor fibers associated with it;
- the local monodromy for the irregular fiber restricted to each Milnor fiber;
- the embeddings of the Milnor fibers into a fixed “reference” regular fiber F .

The first two items are local ingredients, while the third is global. We are able to give complete computation of the local ingredients for $n = 2$ (see Theorem 5.1). The remaining problem for $n = 2$ is therefore the third item, although we obtain enough constraints that the complete topology can be sometimes be deduced.

We use the Briançon polynomial as an illustrative example. In this case our general results quickly yield the previous homological monodromy computations of Artal-Bartolo, Cassou-Nogues, and Dimca [1] and Dimca and Nemethi [6]. Since our computations are geometric, we obtain sharper information (action on the intersection form, etc.). In fact, our computations strongly suggest a candidate description for the complete topology. However, this description remains conjectural, so the example illustrates both the strengths and current limitations of our approach.

1991 *Mathematics Subject Classification.* 14H20, 32S50, 57M25.

This research was supported by the Australian Research Council.

As in the paper [19], we also give a detailed description on the level of homology. That paper shows that, if f is *good*, that is, it has only isolated singularities and no singularities at infinity, then for $n > 3$ the homological data describes the complete topology. Our results prepare the ground for an extension of this result to the case that there are singularities at infinity (at least if the singularities at infinity are also isolated), by extending the topological model of [19] to allow singularities at infinity.

Before we describe our results in more detail, we say a bit more about the basic set-up.

A fiber can be irregular in two ways:

- it may have singularities;
- it may be “irregular at infinity”: failure of local triviality near the given fiber occurs outside arbitrarily large compact sets.

Of course a fiber can be both singular and irregular at infinity; this will, for instance, always be the case if the fiber has non-isolated singularities. There have been many papers dealing with algebraic conditions that imply regularity at infinity (M-tameness of [14] which asks that the given fiber and all nearby fibers be transverse to sufficiently large spheres; ρ -regularity of [26] and [27] which generalizes this to allow non-round spheres; the stronger t-regularity of [23], equivalent to the “Malgrange condition” of [22]). For $n = 2$ these conditions are all equivalent to regularity at infinity (see [8], [27]), but in higher dimensions they are not mutually equivalent. For our purposes the weakest concept of irregularity at infinity, namely the topological one given above, suffices.

In [18] we described results that hold under no conditions on singularities. As already mentioned, we will here be particularly interested in fibers which have only isolated singularities, but no restriction on singularities at infinity. There have been several recent studies of polynomial maps for which the singularities at infinity are also restricted to be isolated in an appropriate sense (e.g., [1], [3], [4], [23], [20], [21]). However most of our results are new even for this case. In particular, the second part of this paper deals only with the case of dimension $n = 2$, in which case singularities at infinity are always isolated.

At an irregular fiber there is a loss of topology compared with the regular fiber. For an isolated singularity the change in topology is captured by the Milnor fiber [13] of the singularity. If f is “good” (no singularities at infinity) then these Milnor fibers account for all the topology of the regular fiber in a way that is made precise by Neumann and Rudolph [19].

For a singularity at infinity there is a “Milnor fiber at infinity,” first described by Suzuki [24] for $n = 2$. One point of this paper is to extend the theory of [19] to encompass the Milnor fibers at infinity also, and to show that the new ingredients — the topology of the singularities at infinity of an irregular fiber, as encoded by the Milnor fibers at infinity and the monodromy maps on these Milnor fibers — are recoverable for $n = 2$ in full from the link at infinity of the irregular fiber.

2. HOMOLOGICAL RESULTS

To clarify what we mean by “loss of topology at an irregular fiber” we start with a simple homological result which is true under no assumption on f .

Definition 2.1. For any fiber $f^{-1}(c)$ of $f: \mathbb{C}^n \rightarrow \mathbb{C}$ choose ϵ sufficiently small that all fibers $f^{-1}(c')$ with $c' \in D_\epsilon^2(c) - \{c\}$ are regular ($D_\epsilon^2(c)$ is the closed disk of radius ϵ about c) and let $N(c) := f^{-1}(D_\epsilon^2(c))$. Let $F = f^{-1}(c')$ be a regular fiber in $N(c)$. Then

$$V_q(c) := \text{Ker}(H_q(F; \mathbb{Z}) \rightarrow H_q(N(c); \mathbb{Z}))$$

is the group of *vanishing q -cycles* for $f^{-1}(c)$.

Let Σ be the set of irregular values of f . Choose a regular value c_0 for f and paths γ_c from c_0 to c for each $c \in \Sigma$ which are disjoint except at c_0 . We use these paths to refer homology of a regular fiber near one of the irregular fibers $f^{-1}(c)$ to the homology of the “reference” regular fiber $F = f^{-1}(c_0)$. From now on F will always mean this particular regular fiber.

Theorem 2.2 ([3], [18]). *For $q > 0$ the maps $V_q(c) \rightarrow H_q(F; \mathbb{Z})$ induce an isomorphism*

$$\bigoplus_{c \in \Sigma} V_q(c) \cong H_q(F; \mathbb{Z}).$$

Moreover, the map $H_q(F; \mathbb{Z}) \rightarrow H_q(N(c); \mathbb{Z})$ with kernel $V_q(c)$ is surjective, so $H_q(N(c); \mathbb{Z}) \cong \bigoplus_{c' \in \Sigma - \{c\}} V_q(c')$. \square

Thus the group of vanishing cycles measures homologically the “loss of topology” at an irregular fiber, and these groups account for all the homology of the regular fiber.

We now restrict to a fiber $f^{-1}(c)$ with at most isolated singularities (but possibly singular at infinity). The “nonsingular core” of $f^{-1}(c)$ is obtained by intersecting $f^{-1}(c)$ with a very large ball and then removing small regular neighborhoods of its singularities. More precisely, there is a radius $R(c)$ such that for any $r \geq R(c)$ the sphere $S_r^{2n-1} \subset \mathbb{C}^n$ of radius r about the origin intersects $f^{-1}(c)$ transversally. Choose any $r \geq R(c)$ and denote $F^{co}(c) := f^{-1}(c) \cap D_r^{2n}(0)$, where $D_r^{2n}(0)$ is the disk of radius r about the origin in \mathbb{C}^n . This $F^{co}(c)$ is the *compact core* of the fiber $f^{-1}(c)$. The fiber $f^{-1}(c)$ is topologically the result of adding an open collar to the boundary of $F^{co}(c)$. Any singularities of f on $f^{-1}(c)$ lie on $F^{co}(c)$ and we remove small open regular neighborhoods of these singularities to form a boundaryed $2n$ -manifold $F^{ns}(c)$, the *non-singular core* of $f^{-1}(c)$.

There may be boundary components of $F^{co}(c)$ outside of which the topology of nearby fibers of f is the same as that of $f^{-1}(c)$, in the sense that f restricted to the appropriate component of $f^{-1}(D_\delta^2(c)) \cap (\mathbb{C}^n - \overset{\circ}{D}_r^{2n}(0))$ gives a locally trivial fibration for $r \geq R(c)$ and δ sufficiently small. We

call such boundary components *regular* and call the other boundary components of $F^{co}(c)$ *irregular*. Thus $f^{-1}(c)$ is regular at infinity if and only if all boundary components of $F^{co}(c)$ are regular.

By standard arguments (see Section 4) we can embed

$$\phi: F^{ns}(c) \times D_\epsilon^2(c) \hookrightarrow \mathbb{C}^n$$

(if ϵ is small enough) so that $\phi(x, c) = x$ for $x \in F^{ns}(c)$ and $f \circ \phi$ is the projection to $D_\epsilon^2(c)$. By restricting ϕ to $F^{ns}(c) \times \{c'\}$ we thus get an embedding of $F^{ns}(c)$ into a nearby regular fiber $F' = f^{-1}(c')$ of f . The complement $F' - \mathring{F}^{ns}(c)$ then consists of the disjoint union of the Milnor fibers of the singularities of f on $f^{-1}(c)$ and certain non-compact pieces. These non-compact pieces will be half-open collars on the regular boundary components of $F^{co}(c)$ and other pieces which meet $F^{ns}(c)$ at irregular boundary components of $F^{co}(c)$. We call the latter the *Milnor fibers at infinity* for $f^{-1}(c)$.

Terminology. By *Milnor fibers of f* we will mean all Milnor fibers of isolated singularities of f and all Milnor fibers at infinity. If we want to emphasize that a Milnor fiber is not at infinity we will call it a *finite Milnor fiber*. Let $F_1(c), \dots, F_{s_c}(c)$ and $F_{s_c+1}(c), \dots, F_{t_c}(c)$ be all the Milnor fibers at infinity respectively finite Milnor fibers for $f^{-1}(c)$.

We will consider the Milnor fibers to lie in our standard regular fiber F , by transporting the fiber $F' = f^{-1}(c')$ along the path γ_c . Topologically, the fiber $f^{-1}(c)$ results from F by collapsing each finite Milnor fiber to a point and removing each Milnor fiber at infinity. This is the sense in which the Milnor fibers capture the loss of topology of the fiber $f^{-1}(c)$. We can use the local monodromy to relate this to vanishing cycles.

For each irregular fiber $f^{-1}(c)$, by transporting a nearby regular fiber F' in a small loop around the fiber $f^{-1}(c)$ we get a local monodromy map $F' \rightarrow F'$. By using the path γ_c to refer this monodromy to the reference regular fiber $F = f^{-1}(c_0)$ we consider it as a map $h(c): F \rightarrow F$. This monodromy map is well defined up to isotopy.

If $f^{-1}(c)$ has isolated singularities, the local monodromy $h(c): F \rightarrow F$ can be normalized to be the identity on the image in F of the non-singular core of $f^{-1}(c)$ (use the above embedding $\phi: F^{ns}(c) \times D^2 \hookrightarrow \mathbb{C}^n$). Thus, $h(c)$ restricts to a local monodromy map on each Milnor fiber $F_i(c)$. We denote this local monodromy map

$$h(c): F_i(c) \rightarrow F_i(c)$$

also by $h(c)$, or simply h .

This map is the identity on $\partial F_i(c)$, so it induces a map in homology called the *variation* (introduced by [12], but with different sign convention)

$$\text{var}: H_q(F_i(c), \partial F_i(c)) \rightarrow H_q(F_i(c)),$$

obtained by taking a relative cycle C to the closed cycle $C - h_{\sharp}C$. Let

$$(v_i)_q: H_q(F_i(c), \partial F_i(c)) \rightarrow H_q(F)$$

be the composition of variation with the map $H_q(F_i(c)) \rightarrow H_q(F)$ induced by inclusion.

Theorem 2.3. *For $q \geq 1$ the maps $(v_i)_q: H_q(F_i(c), \partial F_i(c)) \rightarrow H_q(F)$ are injective and induce an isomorphism*

$$\bigoplus_{i=1}^{t_c} H_q(F_i(c), \partial F_i(c)) \xrightarrow{\cong} V_q(F)$$

to the subgroup $V_q(F) \subset H_q(F)$ of vanishing cycles.

We will prove this theorem in section 4. We first refine it and Theorem 2.2 by describing how monodromy, intersection form, and Seifert form relate to these sum decompositions of homology.

3. MONODROMY AND SEIFERT FORM IN HOMOLOGY

Theorem 3.1. *With respect to the sum decomposition in Theorem 2.2 the map in homology induced by the local monodromy $h(c)$ has the form*

$$\begin{pmatrix} I & 0 & \dots & 0 & 0 & \dots & 0 \\ \vdots & \vdots & & & & & \vdots \\ * & * & \dots & h_c & * & \dots & * \\ \vdots & \vdots & & & & & \vdots \\ 0 & 0 & \dots & 0 & 0 & \dots & I \end{pmatrix}$$

where h_c is the restriction of $H_*(h(c))$ to $V_q(c)$.

If $f^{-1}(c)$ has only isolated singularities, then h_c respects the sum decomposition of Theorem 2.3 and thus has block form

$$\begin{pmatrix} h_{c,1} & 0 \dots & 0 & \\ 0 & h_{c,2} \dots & 0 & \\ \vdots & \vdots & & \vdots \\ 0 & 0 & \dots & h_{c,t_c} \end{pmatrix}$$

where $h_{c,i}$ is induced by the local monodromy $h(c): F_i(c) \rightarrow F_i(c)$.

The *link at infinity* of a fiber $f^{-1}(c)$ with isolated singularities is the link $(S^{2n-1}, S^{2n-1} \cap f^{-1}(c))$, where S^{2n-1} is any sphere around the origin of radius greater than the number $R(c)$ mentioned above. For a regular fiber this link is independent, up to equivalence, of the choice of fiber and is called the *regular link at infinity* for f . A standard construction shows that a Seifert surface of this regular link at infinity (S^{2n-1}, L_{reg}) is diffeomorphic to the compact core F^{co} of a regular fiber (for $n = 2$ this gives the minimal Seifert surface, and this minimal Seifert surface is unique, see [16]).

The Seifert linking form $H_q(F^{co}) \otimes H_{2n-2-q}(F^{co}) \rightarrow \mathbb{Z}$ on the homology of a Seifert surface is a useful invariant of a link.

For each $F_i(c)$ we have a form:

$$(1) \quad \begin{aligned} (L_{c,i})_q: H_q(F_i(c), \partial F_i(c)) \otimes H_{2n-2-q}(F_i(c), \partial F_i(c)) &\rightarrow \mathbb{Z}, \\ \alpha \otimes \beta &\mapsto \text{var}(\alpha) \cdot \beta, \end{aligned}$$

where the dot represents intersection form

$$H_q(F_i(c)) \otimes H_{2n-2-q}(F_i(c), \partial F_i(c)) \rightarrow \mathbb{Z}.$$

Theorem 3.2. *Suppose f has only isolated singularities, so Theorems 2.2 and 2.3 give a direct sum decomposition*

$$\bigoplus_{c \in \Sigma} \bigoplus_{i=1}^{t_c} H_q(F_i(c), \partial F_i(c)) \xrightarrow{\cong} H_q(F) \cong H_q(F^{co}).$$

If we order the set Σ so that the paths γ_c , $c \in \Sigma$, depart the point c_0 in anti-clockwise order, then with respect to this direct sum decomposition the Seifert form of the regular link at infinity has lower triangular block form, with diagonal blocks given by the forms $L_{c,i}$ of (1), and with off-diagonal blocks equal to zero for pairs of summands with the same c :

$$\begin{pmatrix} \dots & 0 & 0 & \dots & 0 & 0 & \dots & 0 \\ \vdots & \vdots & & & & & & \vdots \\ * & * & \dots & L_{c,1} & 0 & \dots & 0 & 0 & \dots & 0 \\ * & * & \dots & 0 & L_{c,2} & \dots & 0 & 0 & \dots & 0 \\ * & * & \dots & \vdots & \vdots & & \vdots & 0 & \dots & 0 \\ * & * & \dots & 0 & 0 & \dots & L_{c,t_c} & 0 & \dots & 0 \\ \vdots & \vdots & & & & & & & & \vdots \\ * & * & \dots & * & * & \dots & * & & & * \end{pmatrix}$$

If f is good, that is, there are no Milnor fibers at infinity, these results are in [19] in slightly different formulation, as follows. The variation map $\text{var}: H_q(F_i(c), \partial F_i(c)) \rightarrow H_q(F_i(c))$ is an isomorphism for the Milnor fiber of an isolated singularity¹. Moreover, in this case the homology $H_q(F_i(c))$ vanishes for $q \neq n-1$ by [13]. Thus, we can replace $(v_i)_q$ in Theorem 2.3 by the map $H_{n-1}(F_i(c)) \rightarrow H_{n-1}(F)$ induced by inclusion when $q = n-1$ (and ignore it when $q \neq n-1$). Moreover, in this case the form of (1) is the Seifert form pulled back to $H_*(F_i, \partial F_i)$ via the variation isomorphism. Thus Theorem 2.3 can be formulated in terms of the Seifert forms of the singularities of f , which is the form in which these results were given in [19].

In this case that f is good the Seifert form is a particularly strong invariant (see [19]): the local homological monodromies of Theorem 3.1 are all computable from the the above block decomposition of the Seifert form on

¹This is a general fact about fibered links, see [12].

$H_{n-1}(F)$, and for $n > 3$ the complete topology of $f: \mathbb{C}^n \rightarrow \mathbb{C}$ is determined by this block decomposition of the Seifert form.

To describe further relations on the above block decompositions, we suppose the irregular values are numbered c_1, \dots, c_k in the order they occur in Theorem 3.2. We abbreviate h_{c_j} as h_j and write the decompositions of monodromy and Seifert form of Theorems 3.1 and 3.2 as:

$$(2) \quad H_*(h(c_j)) = \begin{pmatrix} I & 0 & \dots & 0 & 0 & \dots & 0 \\ \vdots & & & & & & \vdots \\ 0 & 0 & \dots & I & 0 & \dots & 0 \\ h_{j1} & h_{j2} & \dots & h_{j,j-1} & h_j & \dots & h_{jk} \\ \vdots & & & & & & \vdots \\ 0 & 0 & \dots & 0 & 0 & \dots & I \end{pmatrix}$$

$$(3) \quad L = \begin{pmatrix} L_1 & 0 & \dots & 0 & 0 & \dots & 0 \\ L_{21} & L_2 & \dots & 0 & 0 & \dots & 0 \\ \vdots & & & & & & \vdots \\ L_{j1} & L_{j2} & \dots & L_j & 0 & \dots & 0 \\ \vdots & & & & & & \vdots \\ L_{k1} & L_{k2} & \dots & l_{kj} & \dots & \dots & L_k \end{pmatrix}.$$

As described above, h_j and L_j may decompose further as the block sums of the $h_{c_j,i}$ respectively $L_{c_j,i}$, $i = 1, \dots, t_{c_j}$.

It is a standard result that the intersection form S on $H_*(F)$ may be written

$$S = L - L^t$$

where L is the Seifert form discussed above, and L^t is the appropriate graded transpose, $L^t(x, y) = (-1)^{(p+1)(q+1)}L(y, x)$ if $x \in H_q(F)$ and $y \in H_p(F)$ (see, e.g., [7]; in [19] this formula is mistakenly written $S = L + L^t$, and the second instance of $(-1)^{(s+1)(n-s)}$ on the same page 418 should be $(-1)^{s+1}$). The intersection form is, of course, preserved by all the local monodromies $h(c_j)$. The Seifert form, on the other hand, is only preserved by the ‘‘monodromy at infinity’’ $h(\infty) = h(c_k)h(c_{k-1}) \dots h(c_1)$. There are, nevertheless, some relationships between local monodromy and Seifert form which can give useful constraints. The following generalizes Theorem 3.5 of [19].

Theorem 3.3. *With notation as above,*

$$\begin{aligned} L_j h_j &= L_j^t, \\ L_i h_{ij} &= L_{ji}^t && \text{for } i < j, \\ L_i h_{ij} &= -L_{ij} && \text{for } i > j. \end{aligned}$$

This theorem, in fact, implies all the obvious constraints between Seifert form and monodromy, such as the fact that $S = L - L^t$ is preserved by the local monodromies, as well as the relation $LH_*(h(\infty)) = L^t$, discussed below in the proof of this theorem.

4. THE TOPOLOGICAL MODEL

In this section we will prove the results of sections 2 and 3.

Assume that $f^{-1}(c)$ has just isolated singularities. We first describe a topological model for the set $N(c) = f^{-1}(D_c^2(c))$ of Definition 2.1.

Let $\hat{F}(c)$ be the result of removing the interiors of the Milnor fibers $F_i(c)$, $i = 1, \dots, t_c$, from F . Topologically, $\hat{F}(c)$ results by gluing half-open collars on the regular boundary components of $F^{ns}(c)$. The local monodromy map $h(c): F \rightarrow F$ can therefore be taken to be the identity on $\hat{F}(c)$.

Define

$$N_0 := (\hat{F}(c) \times D^2) \cup_{\psi} (F \times_{h(c)} S^1) \times I,$$

where $F \times_{h(c)} S^1$ is the mapping torus for the local monodromy map $h(c): F \rightarrow F$ and ψ is the embedding

$$\psi: \hat{F}(c) \times S^1 = \hat{F}(c) \times_{h(c)} S^1 \rightarrow (F \times_{h(c)} S^1) \times \{0\} \subset (F \times_{h(c)} S^1) \times I,$$

(See Fig. 1). The boundary of N_0 is the disjoint union of $(t_c + 1)$ pieces:

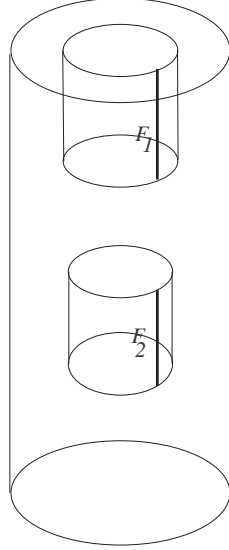


FIGURE 1. Schematic picture of N_0 . Here F_1 is a Milnor fiber at infinity, F_2 a finite Milnor fiber.

$$\begin{aligned} \partial N_0 &= ((F \times_{h(c)} S^1) \times \{1\}) \cup \bigcup_{i=1}^{t_c} ((F_i(c) \times_{h(c)} S^1) \cup (\partial F_i(c) \times D^2)) \\ &= \partial_0 N_0 \cup \bigcup_{i=1}^{t_c} \partial_i N_0 \quad (\text{notation}). \end{aligned}$$

When $F_i(c)$ is a finite Milnor fiber, that is $s_{c+1} \leq i \leq t_c$,

$$\partial_i N_0 = (F_i(c) \times_{h(c)} S^1) \cup (\partial F_i(c) \times D^2) \cong S^{2n-1}$$

is a standard picture of the sphere with its Milnor fibration for the link of the singularity in question (see e.g., [19]). Let N be the result of pasting balls D^{2n} to N_0 along these spheres $\partial_i N_0$ for $i = s_{c+1}, \dots, t_c$.

Proposition 4.1. *N is a partial compactification of $N(c)$ in the following sense: $N(c)$ is homeomorphic² to the result of removing from N all boundary components except the “outer” boundary component $\partial_0 N = F \times_{h(c)} S^1$.*

Proof. If D_i be a small enough ball around the i -th singularity of $f^{-1}(c)$ for $i = s_{c+1}, \dots, t_c$ then $f^{-1}(c)$ is transverse to each ∂D_i and also to $\partial D_r^{2n}(0)$. By compactness, there exists ϵ so that $f^{-1}(c')$ is also transverse to each of these spheres for $|c' - c| \leq \epsilon$. Let $D_0 = D_r^{2n}(0) - \bigcup_{i=1}^{s_c} \mathring{D}_i$ and $X = f^{-1}(D_\epsilon^2(c)) \cap D_0$. Then $f|_X$ is a submersion of a compact manifold with boundary, so by Ehresmann’s theorem (see, e.g., [10]) it is a locally trivial fibration. Since it is a fibration over a disk it is a trivial fibration, so $X \cong F^{ns}(c) \times D_\epsilon^2(c)$. This gives the embedding $\phi: F^{ns}(c) \times D_\epsilon^2(c) \hookrightarrow \mathbb{C}^n$ used in the definition of Milnor fibers at infinity. We can extend ϕ to the collars outside the regular boundary components of $F^{ns}(c)$ (by definition of regular boundary components) to get $\phi: \hat{F}(c) \times D_\epsilon^2(c) \hookrightarrow \mathbb{C}^n$ compatible with the map f and with the trivial structure of f outside regular boundary components of $F^{ns}(c)$.

Let $A = D_\epsilon^2(c) - \mathring{D}_{\epsilon/2}^2(c)$. Then it is clear that $X \cup f^{-1}A$ is diffeomorphic to N_0 so we will identify N_0 with this subset $X \cup f^{-1}A$ of $N(c)$. The closure of $N(c) - N_0$ consists of t_c pieces, of which the last $t_c - s_c$ are “Milnor disk” neighborhoods of the singularities of $f^{-1}(c)$. Gluing these back in to N_0 gives an embedding $N \rightarrow N(c)$, the closure of whose complement consists of pieces Y_i attached at the boundary components $\partial_i N := (F_i(c) \times_{h(c)} S^1) \cup (\partial F_i(c) \times D^2)$ of N for $i = 1, \dots, s_c$. If we show each Y_i is homeomorphic to a half-open collar on $\partial_i N$, then adding Y_i to N has the same effect up to homeomorphism as removing $\partial_i N$, so the proof is complete.

To see Y_i is a collar we can use a standard vector-field argument. Since $f^{-1}(c)$ is transverse to large spheres about 0, we can find a vector-field w in a neighborhood of any point of $f^{-1}(c)$ outside $D_r^{2n}(0)$ so that w is tangent to fibers of f and has radially outward component of magnitude 1. Gluing these local w ’s by a partition of unity, we can find a vector-field w which is defined on all Y_i , is zero off a neighborhood of $f^{-1}(c) \cap Y_i$, is tangent to fibers of f , and has radially outward component of magnitude 1 on $f^{-1}(c) \cap Y_i$ and of magnitude at most 1 elsewhere. We can also assume w is non-zero on the part $\partial F_i(c) \times D_\epsilon^2$ of ∂Y_i .

²We will prove homeomorphism, but using standard angle straightening arguments, cf [10], one can get a diffeomorphism.

Let v_0 be the inward radial vector-field $v_0(x, y) = -(x, y)$ on D_ϵ^2 . Again, by gluing local choices by a partition of unity, we can find a vector-field v on Y_i whose image under f is v_0 , which is tangent on the part $\partial F_i(c) \times D_\epsilon^2$ of ∂Y_i , and which has globally bounded magnitude.

The sum $v + w$ is then a vector-field on Y_i whose flow-lines all lead in backwards time to ∂Y_i and intersect ∂Y_i transversally, and whose forward flow lines continue for infinite time. Integrating the vector-field from ∂Y_i thus gives a homeomorphism of Y_i with $\partial Y_i \times [0, \infty)$, completing the proof. \square

Lemma 4.2. *If N_0 is constructed as for the above proposition then $V_q(c) = \ker(H_q(F) \rightarrow H_q(N_0))$ for $q = 1, \dots, 2n - 3$ and $V_q(c) = 0$ otherwise. Moreover, $H_q(F) \rightarrow H_q(N_0)$ is surjective for $q \neq 2n - 1$.*

Proof. In the previous proof we identified N_0 with a subset of $N(c)$ in such a way that $N(c)$ differs from N_0 by closing some S^{2n-1} boundary components by disks and adding collars to some other boundary components. It follows that the homology of $N(c)$ and N_0 differ only in degree $2n - 1$. Since $V_q(c)$ vanishes if q is not in the range $1, \dots, 2n - 3$, the lemma follows from Theorem 2.2. \square

Proof of Theorem 2.3. The above lemma implies that $V_q(c) \cong H_{q+1}(N_0, F)$ by an isomorphism that fits in a commutative diagram:

$$\begin{array}{ccccccc} 0 & \longrightarrow & H_{q+1}(N_0, F) & \longrightarrow & H_q(F) & \longrightarrow & H_q(N_0) \longrightarrow 0 \\ & & \downarrow \cong & & \parallel & & \parallel \\ 0 & \longrightarrow & V_q(c) & \longrightarrow & H_q(F) & \longrightarrow & H_q(N_0) \longrightarrow 0 \end{array}$$

We identify N_0 with a subset of $N(c)$ as in the proof of Proposition 4.1. Thus f maps N_0 to the disk $D_\epsilon^2(c)$. Moreover, N_0 is the union of the outer shell $N_{out} := f^{-1}(A)$, where $A = D_\epsilon^2(c) - \overset{\circ}{D}_{\epsilon/2}^2(c)$, and an inner core $N_{inn} = \overline{N_0 - N_{out}}$ isomorphic to $\hat{F}(c) \times D_{\epsilon/2}^2(c)$.

Express the disk $D_\epsilon^2(c)$ as the union of two half-disks D_-^2 and D_+^2 by cutting along a diameter. Let N_- and N_+ be the parts of N_{out} that lie over D_- and D_+ and put $N_1 := N_- \cup N_{inn}$. We have

$$N_0 = N_+ \cup N_1,$$

with

$$\begin{aligned} N_+ &\cong F \times I \times I, \\ N_1 &\cong F \times I \times I \cup_{\hat{F}(c) \times I \times \{0\}} \hat{F}(c) \times D^2. \end{aligned}$$

Thus N_1 has $F \times I \times I$ as a deformation retract and the pair $(N_+, N_+ \cap N_1)$ has its intersection with $F \times I \times \{0\}$ (isomorphic to $(F \times I, (F \times \partial I) \cup \hat{F}(c) \times I)$) as a deformation retract. In particular, we see that each of the following

maps induces an isomorphism in homology, since they are, respectively, a homotopy equivalence, an excision map, and a homotopy equivalence:

$$\begin{aligned} (N_0, F) &\hookrightarrow (N_0, N_1) \\ (N_+, N_+ \cap N_1) &\hookrightarrow (N_0, N_1) \\ (F \times I, (F \times \partial I) \cup (\hat{F}(c) \times I)) &\hookrightarrow (N_+, N_+ \cap N_1). \end{aligned}$$

Since

$$(F \times I, (F \times \partial I) \cup (\hat{F}(c) \times I)) = (F, \hat{F}(c)) \times (I, \partial I),$$

we get a homology isomorphism

$$H_{q+1}(N_0, F) \cong H_{q+1}((F, \hat{F}(c)) \times (I, \partial I)).$$

The Künneth theorem thus gives

$$H_{q+1}(N_0, F) \cong H_q(F, \hat{F}(c)) \otimes H_1(I, \partial I) = H_q(F, \hat{F}(c)).$$

Summarizing, we have an isomorphism

$$H_q(F, \hat{F}(c)) \cong V_q(c).$$

The composition $H_q(F, \hat{F}(c)) \xrightarrow{\cong} V_q(c) \rightarrow H_q(F)$ is the variation map (up to sign). Indeed, for the isomorphism $H_q(F, \hat{F}(c)) \rightarrow H_{q+1}(N_0, N_1)$, a relative cycle C is taken to a relative cycle $C \times I$, mapped by $C \times I \rightarrow F \times I \times \{0\} \subset N_+ \subset N_0$ (we are identifying N_+ with $F \times I \times I$). We are interested in the boundary of this cycle as a cycle for $H_q(N_1) \cong H_q(F)$. When we retract N_1 to F , the subset of $N_+ \cap N_1$ given by $\partial(F \times I \times \{0\})$ maps to F by the identity on one component and by h on the other. The resulting cycle in F thus represents $\pm \text{var}([C])$.

Theorem 2.3 now follows because $H_q(F, \hat{F}(c)) \cong \bigoplus_{i=1}^{t_c} H_q(F_i, \partial F_i)$ by excision. \square

Proof of Theorem 3.1. The first part of Theorem 3.1 just says that the image $\text{Im}(H_q(h(c)): H_q(F) \rightarrow H_q(F))$ is contained in $V_q(c)$, which is part of Theorem 1.4 of [18] (it is also proved in section 2 of [6]). The second part of Theorem 3.1 is immediate from the above proof of Theorem 2.3. \square

Proof of Theorem 3.2. We first recall from [19] (see also [16]) how the Seifert linking form for the regular link at infinity can be defined on $H_q(F^{co})$. Let D^2 be a large disk in \mathbb{C} which contains all $c \in \mathbb{C}$ for which $f^{-1}(c)$ is either singular or fails to be M-tame at infinity (in the sense of [14], see also [27]; there are finitely many such c and they include all irregular values of f). Then there is a radius R so that for any $r \geq R$ the boundary of the disk $D_r^{2n}(0)$ intersects all fibers $f^{-1}(t)$ with $t \in \partial D^2$ transversally. Then $D := f^{-1}(D^2) \cap D_r^{2n}(0)$ is homeomorphic to D^{2n} . The embedding of $F^{co} \in \partial D$ as $f^{-1}(t) \cap D$ with $t \in \partial D^2$ gives a Seifert surface for the regular link at infinity. Let F_+^{co} be a neighboring copy of F^{co} , obtained by replacing t by a

nearby point t_+ of ∂D^2 . If a is a cycle for homology $H_q(F^{co})$, let a_+ be a copy of the cycle in F_+^{co} . The Seifert form is the form

$$H_q(F^{co}) \otimes H_{2n-2-q}(F^{co}) \rightarrow \mathbb{Z}, \quad a \otimes b \mapsto \ell(a_+, b),$$

where ℓ is linking number in $S^{2n-1} = \partial D$. It can be computed (up to a sign which depends on conventions; following [7] and [19] the sign is $(-1)^{q+1}$) by letting a_+ and b bound chains A_+ and B in D and taking the intersection number $A_+ \cdot B$.

We now choose our base point c_0 for which $f^{-1}(c_0)$ is our ‘‘standard’’ regular fiber to be the above point t , so we have paths γ_c (as chosen before Theorem 2.3) from t to the irregular values c . We can assume these paths run in the disk D^2 .

Suppose that we have a homology class $[a]$ in the image of the map $v_i(c): H_*(F_i(c), \partial F_i(c)) \rightarrow H_*(F)$. Here, we will consider, for the moment, F to be a regular fiber $f^{-1}(c')$ with $c' \in \partial D_\epsilon^2(c)$, so F is on $\partial N(c)$. We write the cycle a as $\text{var}(\alpha)$ with α a relative cycle in $(F_i, \partial F_i)$. By transporting F_i around the circle $\partial D_\epsilon^2(c)$ we obtain a map of $\alpha \times I$ to $F_i \times_h S^1 \subset \partial N(c)$. The boundary of this chain $\alpha \times I$ consists of the union of α , $h(\alpha)$, and $\partial\alpha \times I$. The part $\partial\alpha \times I$ bounds a mapping of $\partial\alpha \times D_\epsilon^2(c)$ mapping to $\partial F_i \times D_\epsilon^2(c) \subset N(c)$, so we can glue this to $\alpha \times I$ to get a chain A_0 in $N(c)$ with boundary ∂A_0 representing $\text{var}(\alpha) = a$ mapping to F .

If we want a be a cycle for homology of our standard fiber $F = f^{-1}(t)$ we glue onto the above A_0 a copy of $a \times I$ mapping into $f^{-1}(\gamma_c)$. We call the resulting chain A . Note that A_0 lies completely in the ‘‘shell’’ $(F_i \times_h S^1) \cup (\partial F_i \times D_\epsilon^2(c) \subset N_0 \subset N(c)$. We can also construct A_0 in a smaller shell obtained by replacing ϵ by $\epsilon/2$ and removing a thin collar from ∂F_i . We denote the version of A constructed this way by A^{thin} .

Suppose now the two homology classes $[a], [b]$ are in the image of the map $v_i(c): H_*(F_i(c), \partial F_i(c)) \rightarrow H_*(F)$, where F is now our standard regular fiber. We can assume they both lie in F^{co} , since F retracts to F^{co} . We can then make b bound a cycle B as above. We can also make a_+ bound a cycle A_+^{thin} constructed as above but using a path $(\gamma_c)_+$ running parallel to γ_c to a point on $\partial D_{\epsilon/2}^2(c)$. This path runs through a point c'_+ next to c on $\partial D_\epsilon^2(c)$. The chains A_+^{thin} and B intersect only in the fiber $f^{-1}(c'_+)$ and the intersection number $A_+^{\text{thin}} \cdot B$ is, up to sign, the intersection number in $f^{-1}(c')$ of a and β . (See Fig. 2.) With standard sign conventions, the sign is in fact $+1$ (this is most easily checked by using the standard formulae $L^t = LH$ and $S = L - L^t$ relating Seifert form L , intersection form S and monodromy H , since for a knot the relationship to be proved is $L(I - H) = S$). This proves the claim of Theorem 3.2 about the diagonal blocks of the Seifert form. The claim about vanishing of appropriate off-diagonal blocks is the same as the corresponding proof in [19], as suggested by Fig. 3. \square

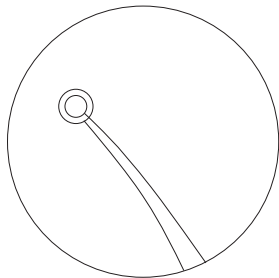


FIGURE 2

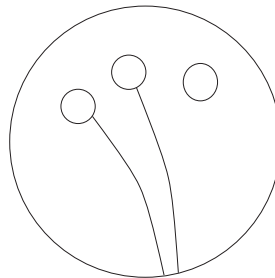


FIGURE 3

Proof of Theorem 3.3. Let M be a 0-codimensional submanifold (with boundary) of the sphere S^m and suppose M is fibered over the circle S^1 with fiber F . Then we can define a Seifert form L and homological monodromy H on the homology of F as for fibered links and the obvious geometric relation $L(x, Hy) = \ell(x_+, Hy) = \ell(x, y_+) = L^t(y, x)$ can be written in matrix form as $LH = L^t$ (this is a well-known relation in the case of fibered links, see, e.g., [7]). If we apply this in the situation of Theorem 3.3 it gives the equation

$$LH_*(h(c_k))H_*(h(c_{k-1})) \dots H_*(h(c_1)) = L^t.$$

An inductive argument, which we omit, shows that this equation is equivalent to the collection of equations of the theorem. \square

5. POLYNOMIALS IN DIMENSION 2

In the remainder of this paper we describe results specific to dimension 2. We assume that $f: \mathbb{C}^2 \rightarrow \mathbb{C}$ has only isolated singularities.

The regular link at infinity determines and is determined by a certain fibered multilink [16], which we will call the *fundamental multilink*. By [17] the link at infinity of any irregular fiber is obtained by splicing additional links onto this multilink; we can call these the *splice components at infinity*. They may decompose further as splices of fibered and non-fibered parts, and the fibered parts are called the *fibered splice components at infinity*.

Theorem 5.1. *For $n = 2$ the Milnor fibers at infinity and their monodromy maps arise as the fibers and monodromy of the fibered splice components at infinity.*

We describe below how the fibered splice components at infinity are determined by the splice diagram for the link. This only depends on the topology of the link (see [9]), so we have the important corollary:

Corollary 5.2. *For $n = 2$ the Milnor fibers at infinity and their monodromy maps are completely determined by the link at infinity of the irregular fibers they belong to (and are effectively computable from their splice diagrams, as described in [9]).* \square

The *splice diagram* of the link at infinity of a complex affine plane curve ([16]), which from the point of view of classical algebraic geometry is simply

an encoding of the Puiseux tree at infinity, also encodes the splice decomposition of the link at infinity ([9]). It is a weighted tree with some leaves drawn as arrowheads to stand for link components of the link. Splicing links corresponds to gluing such diagrams at arrowheads. Conversely, disconnecting a splice diagram by cutting an edge and drawing two arrowheads on the resulting ends corresponds to the inverse operation of splice decomposition. Any link obtainable via repeated splice decomposition is called a “splice component.” Splice components are thus represented by connected subgraphs of the splice diagram.

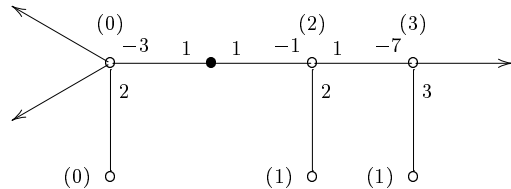
The *fibred splice components at infinity* are the splice components corresponding to the maximal connected subgraphs of the splice diagram having only negative vertex linking weights. The example below will clarify this.

Before proving Theorem 5.1, we illustrate it using the example of the “Briangon polynomial”

$$f(x, y) = x^2(1 + xy)^4 + 3x(1 + xy)^3 + \left(3 - \frac{8}{3}x\right)(1 + xy)^2 - 4(1 + xy) + y.$$

This polynomial was shown to have no finite singularities by Briangon, see [2] where it is also shown that all fibers of f are connected. It has two irregular fibers (over 0 and $-16/9$). The Jordan normal forms for action in homology of the monodromy generators $h(0)$ and $h(-16/9)$ were computed by Artal-Bartolo, Cassou-Nogues, and Dimca [1]. Dimca and Nemethi [6] computed these with respect to a common basis of homology, thus determining the complex monodromy representation for this example. We will show how the splice diagrams make these computations “routine” and give the geometric monodromy rather than just the action on homology. However, as the example will make clear, our approach still falls short of achieving our goal of a practical complete algorithmic description of the topology.

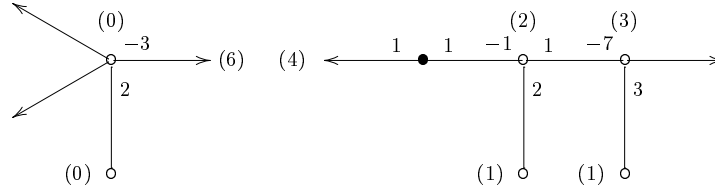
The splice diagrams for the links at infinity of the fibers of f were computed in [2]. The regular splice diagram is as follows, where we have included the linking weights (also called multiplicity weights) at vertices in parentheses:



The fact that vertices with zero linking weights occur is equivalent to each of the following two facts (see [9], [16] and [17]):

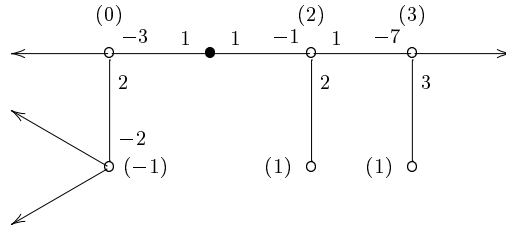
- the regular link at infinity is not a fibred link;
- f has fibers that are irregular at infinity.

We write the link as the splice of the part with zero linking weights and a fibered multilink:



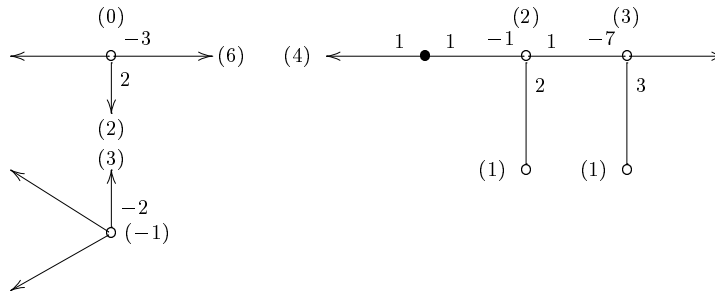
The fibered multilink is the multilink associated with the regular link at infinity for f as described in [16]. We call it the *fundamental multilink* for f . As described there, it is a fibered multilink which determines and is determined by the regular link at infinity. Its fibers are, up to isotopy, the regular fibers of f over the points of a large circle in \mathbb{C} so its fibration gives the monodromy at infinity for f (which is the product of the local monodromies around the irregular fibers). We will return to this later and first examine the irregular fibers.

The Briançon polynomial has irregular fibers $f^{-1}(0)$ and $f^{-1}(-16/9)$. The link at infinity for $f^{-1}(0)$ has splice diagram



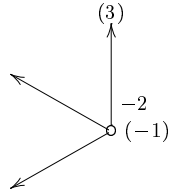
It follows that $f^{-1}(0)$ has Euler characteristic -2 . Since it has 4 boundary components, it is a four-punctured sphere.

We express the link at infinity of this irregular fiber as the splice of the parts with positive, zero, and negative linking weights respectively:



The part with positive linking weights is always the fundamental multilink (see [17]). We call the parts with negative total linking weights (in this case there is just one) the *fibered splice components at infinity*. So the fibered

splice component at infinity is given by the splice diagram:



Its fiber has Euler characteristic -1 and 3 boundary components, so it is a thrice-punctured disk (see Fig. 4). If we remove the boundary component

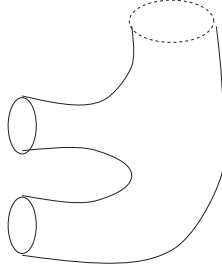


FIGURE 4

marked with a dashed curve (corresponding to the arrowhead where the fibered splice component at infinity splices to the rest of the irregular spliced diagram) we obtain the Milnor fiber at infinity for this irregular fiber. This would be $F_1(0)$ in our earlier notation, but there is just the one Milnor fiber at infinity for $f^{-1}(0)$, so we call it $F(0)$.

The local monodromy for this Milnor fiber is given by the monodromy of the fibered splice component at infinity. The book [9] describes how to compute this monodromy from the splice diagram. We need the monodromy in which the boundary of $F(0)$ (consisting of the two circles at the left of the figure) is fixed. By Theorem 13.5 of [9] it is the result of doing a Dehn twist on an annulus parallel to each of these boundary components. It follows that the variation map

$$\text{var}: \mathbb{Z} \cong H_1(F(0), \partial F(0)) \rightarrow H_1(F(0))$$

takes a generator of $H_1(F(0), \partial F(0))$ to the homology class of the difference of the two boundary components. Following the orientation conventions of [9] the bilinear form occurring in Theorem 3.2 (given by equation (1)) thus has matrix (2).

The regular fiber F is the result of gluing the Milnor fiber at infinity to the irregular fiber (Fig. 5). By Theorem 2.3, the subgroup $V_1(0) \subset H_1(F)$ of vanishing cycles for the fiber $f^{-1}(0)$ is generated by the difference of the two separating curves in this figure. This is fixed by the local monodromy, so the monodromy matrix is (1).

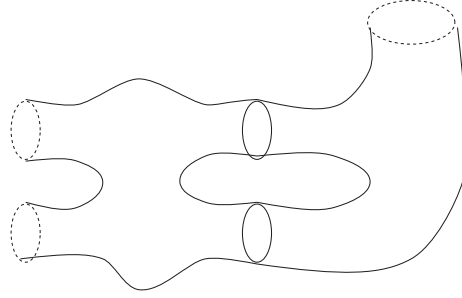


FIGURE 5

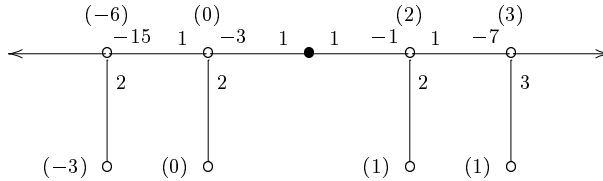
We will number our irregular values $c_1 = -16/9, c_2 = 0$, since this is the ordering Dimca and Nemethi use in [6]. So, in the notation of equations (2) and (3) in section 3 we have

$$(4) \quad L_2 = (2), \quad h_2 = (1),$$

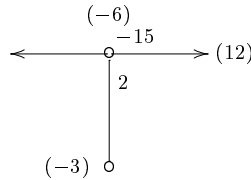
$$(5) \quad H_1(h(c_2)) = \left(\begin{array}{cc|c} I & 0 & \\ \hline h_{21} & h_2 & \end{array} \right) = \left(\begin{array}{ccc|c} 1 & 0 & 0 & 0 \\ 0 & 1 & 0 & 0 \\ 0 & 0 & 1 & 0 \\ \hline p & q & r & 1 \end{array} \right)$$

with $h_{21} = (p, q, r)$ still to be determined.

We now do a similar analysis for the irregular fiber $f^{-1}(-16/9)$. The splice diagram for the link at infinity of this fiber is:



so the irregular fiber $f^{-1}(-16/9)$ has Euler characteristic 0 and is thus an annulus. Moreover, the fibered splice component at infinity for this irregular link at infinity has diagram:



The fiber of this fibered multilink is a thrice-punctured torus (right hand piece of Fig. 6) which glues to the irregular fiber as in Fig. 6 to give a copy of the regular fiber F . We call this Milnor fiber at infinity $F(-16/9)$. The local monodromy on it is isotopic to an order 6 map (because of the linking weight -6) and it exchanges the two boundary components at the right (the circles corresponding to a single edge of the splice diagram of a fibered multilink are always permuted transitively by the monodromy for the fibration). The

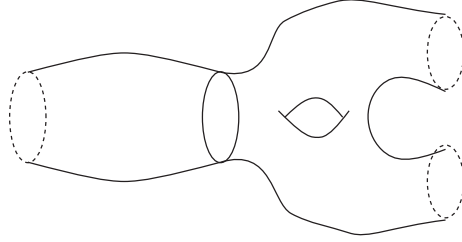


FIGURE 6

local monodromy on F is thus also isotopic to this order 6 map, since F and $F(-16/9)$ just differ by a collar.

Again we can use this description to compute the local monodromy and the block L_1 of the Seifert form. We describe this in greater detail later, but a quick approach is to note that there are exactly two different order 6 transformations of the surface in question with given action on the boundary, differing only in orientation. The correct orientation can be deduced from the boundary twist computations in [9] or by means of the equivariant signature computation of Theorem 5.3 of [15] (as generalized in section 6 of that paper). In any case, with respect to a suitable basis of homology, the answer is:

$$(6) \quad L_1 = \begin{pmatrix} 1 & 1 & 0 \\ 0 & 1 & 0 \\ 0 & 0 & 0 \end{pmatrix}, \quad h_1 = \begin{pmatrix} 0 & -1 & 0 \\ 1 & 1 & 0 \\ 0 & -1 & -1 \end{pmatrix}$$

$$(7) \quad H_1(h(c_1)) = \begin{pmatrix} h_1 & h_{12} \\ 0 & I \end{pmatrix} = \left(\begin{array}{ccc|c} 0 & -1 & 0 & a \\ 1 & 1 & 0 & b \\ 0 & -1 & -1 & c \\ \hline 0 & 0 & 0 & 1 \end{array} \right)$$

with $h_{12} = (a, b, c)^t$ still to be determined.

At this point we can write down the Seifert matrix L as

$$(8) \quad L = \begin{pmatrix} L_1 & 0 \\ L_{21} & L_2 \end{pmatrix} = \left(\begin{array}{ccc|c} 1 & 1 & 0 & 0 \\ 0 & 1 & 0 & 0 \\ 0 & 0 & 0 & 0 \\ \hline x & y & z & 2 \end{array} \right)$$

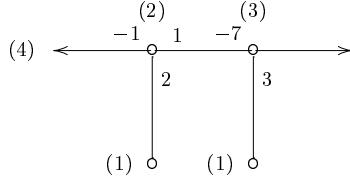
with $L_{21} = (x, y, z)$ still to be determined. However, applying the relations of Theorem 3.3 gives:

$$a + b = x, \quad b = y, \quad 0 = z, \quad 2p = -x, \quad 2q = -y, \quad 2r = -z,$$

so in fact we just have three unknown integers in equations (5), (7), (8), namely p, q, c , and the others are then determined as

$$(9) \quad r = z = 0, \quad x = -2p, \quad y = -2q, \quad a = 2q - 2p, \quad b = -2q.$$

The product of the two local monodromy maps is the monodromy at infinity for the regular fiber. This monodromy at infinity is the monodromy of the fundamental multilink (by the definition of this multilink in [16]), so it can be computed from the splice diagram for this multilink. In our particular case that splice diagram (as an unrooted diagram) is



The fiber of this fibered multilink decomposes according to the splice components determined by the two nodes of this diagram as in Fig. 7, and the

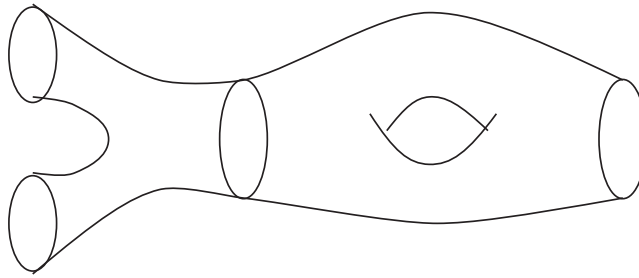


FIGURE 7

monodromy restricted to the left part is isotopic to a map of order 2 and restricted to the right part is isotopic to a map of order 3. The sixth power of this monodromy gives a single Dehn twist on the joining circle by Theorem 13.1 of [9].

This monodromy map in $H_1(F)$ has eigenvalues $-1, 1, e^{\pm 2\pi i/3}$, so its characteristic polynomial is $(t + 1)(t^3 - 1) = t^4 + t^3 - t - 1$. On the other hand, equations (5), (7), and (9) show the monodromy map is

$$\begin{aligned}
 H_1(h(c_2))H_1(h(c_1)) &= \begin{pmatrix} 1 & 0 & 0 & 0 \\ 0 & 1 & 0 & 0 \\ 0 & 0 & 1 & 0 \\ p & q & 0 & 1 \end{pmatrix} \begin{pmatrix} 0 & -1 & 0 & -2p + 2q \\ 1 & 1 & 0 & -2q \\ 0 & -1 & -1 & c \\ 0 & 0 & 0 & 1 \end{pmatrix} \\
 &= \begin{pmatrix} 0 & -1 & 0 & -2p + 2q \\ 1 & 1 & 0 & -2q \\ 0 & -1 & -1 & c \\ q & -p + q & 0 & -2p^2 + 2pq - 2q^2 + 1 \end{pmatrix}.
 \end{aligned}$$

This has characteristic polynomial

$$(t - 1)(t^3 + 2(p^2 - pq + q^2 - 1)(t^2 - t) - 1),$$

so

$$p^2 - pq + q^2 - 1 = 0.$$

This equation has six solutions:

$$(p, q) = \pm(1, 1), \pm(1, 0), \pm(0, 1)$$

with corresponding values

$$(a, b) = \pm(0, -2), \pm(-2, 0), \pm(2, -2).$$

But, by changing our choice of basis on $H_1(F(-16/9))$ by powers of the local monodromy we cycle through these six possibilities, so they are all equivalent. Choosing $(p, q) = (1, 0)$ gives the conclusion:

$$\begin{aligned} H_1(h(c_2)) &= \begin{pmatrix} 1 & 0 & 0 & 0 \\ 0 & 1 & 0 & 0 \\ 0 & 0 & 1 & 0 \\ 1 & 0 & 0 & 1 \end{pmatrix} \\ H_1(h(c_1)) &= \begin{pmatrix} 0 & -1 & 0 & -2 \\ 1 & 1 & 0 & 0 \\ 0 & -1 & -1 & c \\ 0 & 0 & 0 & 1 \end{pmatrix} \\ L &= \begin{pmatrix} 1 & 1 & 0 & 0 \\ 0 & 1 & 0 & 0 \\ 0 & 0 & 0 & 0 \\ -2 & 0 & 0 & 2 \end{pmatrix} \end{aligned}$$

Here c is still undetermined, and we know no way of finding it with our current methods. However, one calculates easily that the isomorphism type of the monodromy representation over \mathbb{C} depends only on the vanishing or not of $3c + 2$, which is non-vanishing since it is not divisible by 3. An equivalent non-vanishing issue arose in the computation of complex monodromy in [6] and was resolved by a more complicated argument.

We have described what can be read directly and easily from the splice diagrams. To complete the information about the global monodromy takes more work, since we must identify the three different pictures of the regular fiber F of Figs. 5, 6, and 7 to fully understand the global picture. It is easy to see that the boundary component at the right of Fig. 7 corresponds to the one at the left in Fig. 6 and one of the ones at the left in Fig. 5. The issue is to determine how the two circles in Fig. 5 lie with respect to the order 6 map of Fig. 6. This would also determine how they lie with respect to the separating circle of Fig. 7. The homology information gives strong hints, but no obvious complete answer. In the next section we give a conjectural answer.

6. A TENTATIVE PICTURE OF THE BRIANÇON TOPOLOGY

Let F denote the three-punctured torus. We will describe explicit maps h_1 and h_2 of F that satisfy all the properties of the local monodromy maps

$h(c_1)$ and $h(c_2)$ for the Briancon polynomial that were computed in the previous section. Namely, h_1 , h_2 , and h_2h_1 are conjugate in the group of orientation preserving diffeomorphisms of F to the maps $h(c_1)$, $h(c_2)$, and $h(\infty)$ of the previous section.

We will represent F as the 2-fold cover of a punctured disk branched at three points, described by branch cuts as in Fig. 8. The inner boundary

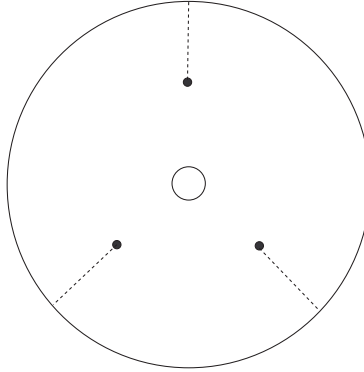


FIGURE 8. F as a 2-fold cover; the dashed lines represent branch cuts

component is thus covered by two boundary components of F and the outer boundary component is double covered by one boundary component of F .

Our map h_1 will be the order 6 map which rotates the picture by one-third of a turn clockwise and exchanges the two branches.

Consider now the curves on F labeled β , β' , δ , as in Fig. 9. The curves β

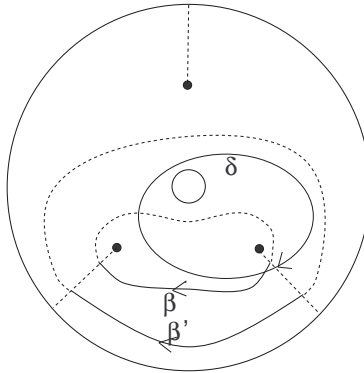


FIGURE 9. The dashed portions of curves lie on the “back” branch of F ; δ is double covered in F

and β' cut F into two pieces of genus zero as in Fig. 5. We therefore define h_2 to be the product of the Dehn twists on these two curves. The curve δ

cuts F into two pieces as in Fig. 7. By drawing a careful picture one finds that the effect of h_2 on $h_1(\delta)$ is to take it to δ , so h_2h_1 takes δ to itself. In fact, h_2h_1 is conjugate to the map $h(\infty)$, with δ playing the role of the separating curve in Fig. 7. This can be seen by drawing careful pictures, but it is also forced by the fact that δ is mapped to itself together with the homology computation below.

Now let α and γ be the curves of Fig. 10 and let γ' be the curve represented

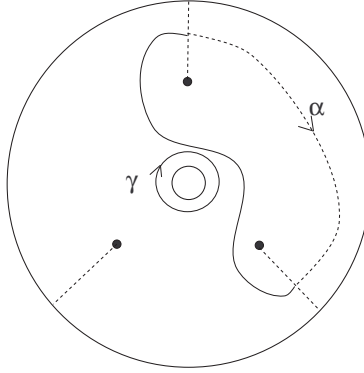


FIGURE 10

by a dashed circle in place of γ (this is the image of γ under h_1). The intersection number $\alpha \cdot \beta$ is 1, so α and β form a basis for the homology $H_1(\overline{F})$ of the closed torus obtained by filling the punctures of F . A basis for the homology of F is therefore given by $\alpha, \beta, \gamma, \gamma'$. However, computing the images of the variation maps for h_1 and h_2 leads to the basis

$$\alpha, \beta, \gamma - \gamma'; \quad \beta + \beta' = 2\beta + \gamma',$$

which we therefore use instead. With respect to this basis it is easily checked that the actions of h_2 and h_1 on homology are by the matrices

$$\begin{pmatrix} 1 & 0 & 0 & 0 \\ 0 & 1 & 0 & 0 \\ 0 & 0 & 1 & 0 \\ 1 & 0 & 0 & 1 \end{pmatrix} \quad \text{and} \quad \begin{pmatrix} 0 & -1 & 0 & -2 \\ 1 & 1 & 0 & 0 \\ 0 & -1 & -1 & -1 \\ 0 & 0 & 0 & 1 \end{pmatrix}.$$

These are the matrices for $H_1(h(c_2))$ and $H_1(h(c_1))$ of the previous section with $c = -1$.

As already stated, we do not know if the above is really the appropriate monodromy. The computation of the previous section implies that the two curves of Fig. 5 are $\beta + r(\gamma - \gamma')$ and $\beta + r(\gamma - \gamma') \pm \gamma'$ in homology for some $r \in \mathbb{Z}$ (and it then follows easily that the c in $H_1(h(c_2))$ is odd: namely $c = -4r - 2 \pm 1$). There are many pairs of disjoint simple closed curves that satisfy this, but the fact that $h(c_2)h(c_1)$ has to fix a separating closed curve and be isotopic to order two and three maps on the resulting pieces of

F seems a very strong constraint, and may well eliminate most or all other possibilities.

7. PROOF OF THEOREM 5.1

We first need to recall some basics about multilinks and splicing. See [9] for details.

For the moment, by a “link” we will understand a pair (Σ, L) consisting of an oriented submanifold L of dimension 1 in a 3-dimensional homology sphere Σ . It is a “knot” if L consists of a single closed curve. Our homology sphere Σ will always be S^3 in applications in this paper, but the discussion of splicing is easier without this restriction.

The *link exterior* for a link (Σ, L) is the manifold with boundary $\Sigma - \mathring{N}(L)$, where $N(L)$ is a (small) closed regular neighborhood of L in Σ .

A *multilink* is a link (Σ, L) with an integer “multiplicity” $m(K)$ assigned to each component K of L , with the convention that reversing the orientation of a component K and simultaneously changing the sign of $m(K)$ gives the same multilink. In other words, the multilink structure is given by a 1-cycle m supported on L . Equivalently, and more conveniently, it is given by the cohomology class $\mu \in H^1(\Sigma - L; \mathbb{Z})$ whose value on a 1-cycle c is the linking number $\ell(m, c)$. A Seifert surface for the multilink is a map of a compact oriented surface S to Σ which maps ∂S to L , is an embedding on $S - \partial S$, and, considered as a 2-chain, has the above 1-cycle m as boundary. If $N(L)$ is a regular neighborhood of L that intersects the Seifert surface S in a collar on ∂S then the surface $S - S \cap \mathring{N}(L)$ in the link exterior $\Sigma - \mathring{N}(L)$ is also called a Seifert surface.

If (Σ_1, K_1) and (Σ_2, K_2) are knots, we form the *splice*

$$\Sigma = \Sigma_1 \overline{K_1 \ K_2} \Sigma_2$$

by pasting together link exteriors of each knot as follows:

$$\Sigma = (\Sigma_1 - \mathring{N}_1) \cup_{\partial} (\Sigma_2 - \mathring{N}_2),$$

where the pasting along boundaries ∂N_1 and ∂N_2 is done so as to match a meridian of K_1 to a longitude of K_2 and meridian of K_2 with longitude of K_1 . A simple homology calculation shows Σ is again a homology sphere.

If K_1 and K_2 are components of links $L_1 \subset \Sigma_1$ and $L_2 \subset \Sigma_2$ and $L = (L_1 - K_1) \cup (L_2 - K_2)$ then we write

$$(\Sigma, L) = (\Sigma_1, L_1) \overline{K_1 \ K_2} (\Sigma_2, L_2),$$

the *splice of (Σ_1, L_1) to (Σ_2, L_2) along K_1 and K_2* .

If (Σ, L) has a multilink structure then we get induced multilink structures on each (Σ_i, L_i) by restricting the cohomology class that defines the multilink structure. Note that, even if the multilink (Σ, L) is a link (all multiplicities are 1), the multiplicities of K_1 and K_2 will in general be different from 1.

Thus decomposing links via splicing leads one naturally into the realm of multilinks.

If (Σ, L) results from splicing two links as above then there is a torus T^2 in the link exterior $\Sigma - \mathring{N}(L)$ along which the splicing occurred. Conversely, suppose (Σ, L) is a link and $T^2 \subset \Sigma - \mathring{N}(L)$ an essential torus (i.e., the induced mapping $\pi_1(T^2) \rightarrow \pi_1(\Sigma - \mathring{N}(L))$ is injective and T^2 is not isotopic to a boundary component of $\Sigma - \mathring{N}(L)$). Then (Σ, L) is the result of a non-trivial splicing operation along this torus: cutting Σ along T^2 gives two homology solid tori, and we obtain Σ_1 and Σ_2 from Σ by replacing each of these homology solid tori in turn by a genuine solid torus.

In this situation, if Σ is S^3 then Σ_1 and Σ_2 are also S^3 . In the following we will start with a link in S^3 and splice decompose it, so we never see homology spheres other than S^3 .

We will study the topology of $f: \mathbb{C}^2 \rightarrow \mathbb{C}$ by intersecting fibers with a large disk in \mathbb{C}^2 . In fact our basic topological object will be a 4-disk \mathbb{D} obtained as follows: take a large disk D^2 that contains all irregular values of f , intersect $f^{-1}(D^2)$ with a very large 4-disk in \mathbb{C}^2 , and then push in “holes” around the fibers that are irregular at infinity as in the models N of Proposition 4.1. See Fig. 11.

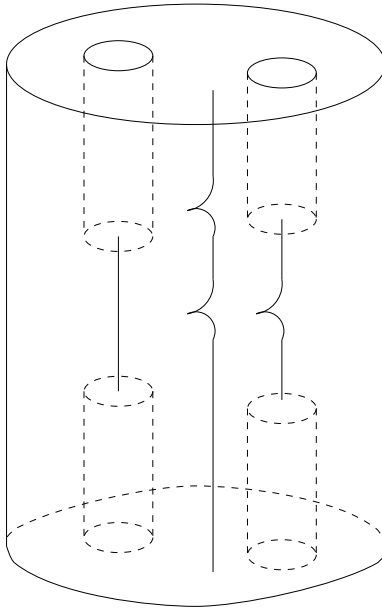


FIGURE 11

We will need to do this carefully to confirm the desired properties of the resulting space. As in [16], it is convenient to use a polydisk $D(q, r) := \{(x, y) \in \mathbb{C}^2 : |x| \leq q, |y| \leq r\}$ for our “very large 4-disk”. We recall Lemma 2.1 of [16]:

Lemma 7.1. *By a linear change of coordinates we may assume $f(x, y)$ is of degree n and of the form $f(x, y) = x^n + f_{n-1}(y)x^{n-1} + \dots + f_0(y)$. We choose s so all irregular values of f lie in the disk $D_s^2(0) \subset \mathbb{C}$. Then for r sufficiently large and q sufficiently large with respect to r the fibers $f^{-1}(t)$ for $t \in \partial D_s^2(0)$ intersect $\partial D(q, r)$ only in the part $|x| < q, |y| = r$, and do so transversely — in fact they intersect each line $y = y_0$ with $|y_0| \geq r$ transversely.*

We sketch a slight modification of the argument in [16]. The fiber $f^{-1}(t)$ fails to be transverse to the line $y = y_0$ if and only if y_0 is the image of a branch point of the projection $f^{-1}(t) \rightarrow \mathbb{C}$ given by the y -coordinate. If $f^{-1}(t)$ is reduced (no multiple components) there will be finitely many such branch points on $f^{-1}(t)$. The locus of such branch points as t varies is an algebraic curve B in \mathbb{C}^2 (given by the equation $\Delta(y, f(x, y)) = 0$, where $\Delta(y, t)$ is the discriminant of the polynomial $f(x, y) - t \in \mathbb{C}[y, t][x]$). A fiber $f^{-1}(c)$ is irregular at infinity if and only if it is not reduced (in which case it has a component in common with B) or if intersection points of B with nearby fibers $f^{-1}(t)$ move off to infinity as t approaches c . Thus $f^{-1}(\partial D_s^2(0)) \cap B$ is compact, and if we choose r large enough that this compact set lies in the domain $|y| < r$ of \mathbb{C}^2 then r does what is desired.

This proof actually shows more. Choose ϵ small enough that the disks $D_\epsilon^2(c)$ about the irregular values of f are pairwise disjoint and lie in the interior of $D_s^2(0)$. Denote $X = D^2 - \bigcup_{c \in \Sigma} \mathring{D}_\epsilon^2(c)$. Then

Scholium. *With notation as above, if the radius r is sufficiently large then the fibers $f^{-1}(t)$ for $t \in X$ intersect each line $y = y_0$ with $|y_0| \geq r$ transversely.*

As described in [16], if r is chosen as in the above Lemma, then

$$D := f^{-1}(D_s^2(0)) \cap \{|y| \leq r\}$$

is a 4-disk in \mathbb{C}^2 . (This can be seen by noting that \mathbb{C}^2 results by gluing $f^{-1}(D_s^2(0)) \cap \{|y| \geq r\}$ to D along part of ∂D and then gluing $f^{-1}(\mathbb{C} - \mathring{D}_s^2(0))$ along the boundary of the result. The first part glued on is a collar because $f^{-1}(D_s^2(0)) \cap \{|y| \geq r\} \rightarrow [r, \infty)$, $(x, y) \mapsto |y|$ is a locally trivial fibration, and the second part is obviously a collar.)

We now assume r' was chosen sufficiently large that all irregular fibers $f^{-1}(c)$, $c \in \Sigma$, are transverse to the lines $y = y_0$ with $|y_0| \geq r'$. In particular, the irregular fibers are transverse to the cylinders $\{|y| = r\}$ with $r \geq r'$. Then assume ϵ was chosen small enough that all fibers $f^{-1}(t)$ with t in $\bigcup_{c \in \Sigma} D_\epsilon^2(c)$ are transverse to the cylinders $\{|y| = r'\}$. Then r is chosen as in the Scholium above.

For each $c \in \Sigma$ the set $f^{-1}(\mathring{D}_\epsilon^2(c)) \cap \{|y| > r'\}$ consists of components $(f^{-1}(\mathring{D}_\epsilon^2(c)) \cap \{|y| > r'\})_i$, $i = 1, \dots, r_c$ corresponding to places where $f^{-1}(c)$ is irregular at infinity, and maybe additional components where

$f^{-1}(c)$ is regular at infinity. Let

$$\mathbb{D} = D - \left(\bigcup_{c \in \Sigma} \bigcup_{i=1}^{r_c} \left(f^{-1}(\mathring{D}_c^2(c)) \cap \{|y| > r'\} \right)_i \right),$$

see Fig. 11 above. The argument of Section 4 easily adapts to show that D results topologically by adding a collar to part of the boundary of \mathbb{D} , so \mathbb{D} is homeomorphic to D^4 .

We will need names for the parts of the boundary of \mathbb{D} . Denote

$$E := f^{-1}(\partial D_s^2(0)) \cap \mathbb{D}, \quad S := \partial \mathbb{D} - \mathring{E}.$$

Then S is the union of the part

$$S_0 := S \cap \{|y| = r\},$$

and $S - \mathring{S}_0$, which is the union of pieces

$$T_i(c) \cong (F_i(c) \times_h S^1) \cup (\partial F_i(c) \times D^2)$$

for $c \in \Sigma$ and $i = 1, \dots, s_c$ (recall that $F_i(c) \times_h S^1$ denotes the mapping torus of the local monodromy on the Milnor fiber $F_i(c)$ at infinity).

Lemma 7.2. *S is a union of solid tori and each $T_i(c)$ is homeomorphic to a solid torus.*

Proof. Let $S' = \partial D - \mathring{E}$. That S' is a union of solid tori was proved in [16]. The argument (due to L. Rudolph) is that for $|y_0| = r$ the intersection $S' \cap \{y = y_0\}$ is transverse and the result is a union of disks by the maximum modulus principle, since it is equivalent to the set $\{x \in \mathbb{C} : |f(x, y_0)| \leq s\}$. On the other hand, $S' \cong S$ by the argument that identifies $D - \mathring{\mathbb{D}}$ with collars on the $T_i(c)$'s, so S is a union of solid tori.

The same argument applies to show the sets $f^{-1}(D_c^2(c)) \cap \{|y| = r\}$ are unions of solid tori for $c \in \Sigma$. But the components of these sets are homeomorphic to the $T_i(c)$'s. \square

The above decomposition of $\partial \mathbb{D}$ gives splice decompositions of the links at infinity of the fibers of f . The basic fact was described earlier in this section: if (S^3, L) is a link and we cut the link exterior $S^3 - \mathring{N}(L)$ into pieces along embedded tori, then this represents (S^3, L) as the result of a splicing operations.

In particular, the piece E of $\partial \mathbb{D}$ is the exterior of a splice component (S^3, L) , where $L \subset S^3 = \partial \mathbb{D}$ is the link consisting of the cores of the solid tori making up S . This splice component is the fundamental multilink for f as described in [16]. The fibration of the the exterior E of this multilink is simply given by the restriction $f|_E$.

We shall see that, possibly after minor modification to eliminate parallel tori, the above splice decomposition of the link at infinity of an irregular fiber of f is as described in Theorem 5.1.

Note that $f|_{S_0}: S_0 \rightarrow X$ is a fibration of S_0 over the punctured disc X with each fiber a union of circles (isotopic to the regular link at infinity of f). We can extend this map over the solid tori $T_i(c)$ to get a Seifert fibration of S . But S is a disjoint union of one or more solid tori and, up to isotopy, the only Seifert fibrations of a solid torus are the standard (p, q) -fibrations in which the core circle is a fiber and the general fiber p -fold covers this core circle (we do not rule out the possibility of $(p, q) = (0, 1)$, called a “generalized Seifert fibration” in [11]³). Thus, each component of $S - \bigcup_i T_i(c)$ is a solid torus with a collection of thinner solid tori removed, all or all but one of which run parallel to fibers of this Seifert fibration, and maybe one running parallel to the core circle.

The link at infinity of an irregular fiber $f^{-1}(c)$ can be seen as the intersection of $f^{-1}(c)$ with $\partial\mathbb{D}$. We thus have a splice decomposition of this link at infinity into:

- the fundamental multilink,
- fibered multilinks based on the pieces $T_i(c)$,
- multilinks with exteriors given by the components of the Seifert fibered piece $S - \bigcup_i T_i(c)$.

The latter will lead to the non-fibered components mentioned in the theorem. However, some components of $S - \bigcup_i T_i(c)$ could be of the form: solid torus minus a thinner solid torus parallel to the core circle, giving a toral annulus $T^2 \times I$. In this case the two torus boundary components of this piece are parallel, so to obtain an irredundant splice decomposition we must omit one of them and absorb this toral annulus as a collar on an adjacent splice component.

To complete the proof of Theorem 5.1 we must show the splice decomposition we have found is as described in that theorem. We do this by examining our construction in terms of a compactification of \mathbb{C}^2 . Since the relationship between the compactification divisor and the splice diagram is already worked out in detail in [9] and [17], this then does what we require.

We extend the polynomial map $f: \mathbb{C}^2 \rightarrow \mathbb{C}$ to a map $\bar{f}: Z \rightarrow \mathbb{C}P^1$ of a smooth compact complex surface Z to $\mathbb{C}P^1$. The compactification divisor $Y := Z - \mathbb{C}^2$ is a union of smooth rational curves with dual intersection graph a tree. A component of Y on which \bar{f} is non-constant is called *horizontal*. A component of Y on which \bar{f} is constant is called *finite* or *infinite* according to the value of \bar{f} on it.

By blowing up if necessary, we can assume that the only singularities of fibers of \bar{f} that occur on Y are normal crossings between components of the fiber and components of Y .

We can encode the topology of Y in the usual way by a plumbing graph. This is a tree, with vertices corresponding to components of Y and edges for intersections between components. It has a weight at each vertex to show the self-intersection number of the corresponding component of Y . We draw

³One can show it cannot occur here, but we do not need this.

arrows at vertices to indicate where fibers of \bar{f} intersect Y . The following diagram, which gives a compactification divisor for the Briancon polynomial, uses solid arrows for the general fiber and dashed respectively dotted arrows for the two irregular fibers. Note that the three curves on the left could be blown down if we only wanted a compactification on which \bar{f} is well defined; they arose from blowing up to resolve a singularity of an irregular fiber on Y .

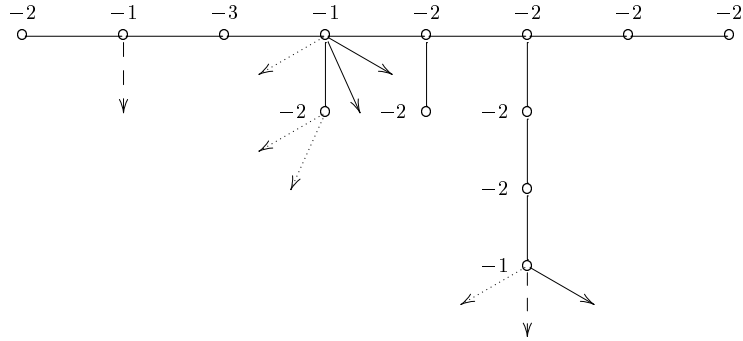


Fig. 12 is a schematic picture of the compactification divisor in this case.

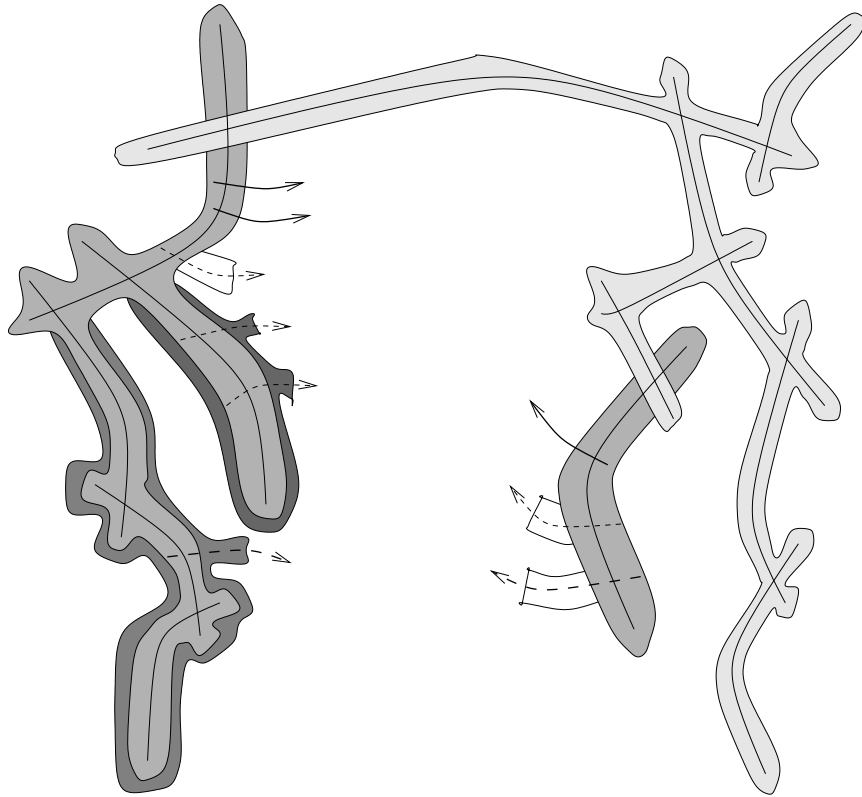


FIGURE 12

We have shaded the domains that are removed in constructing the manifold \mathbb{D} above:

- Removing the lightest shaded region removes everything whose image under \bar{f} lies outside the disk $D_s^2(0)$.
- Removing the next lightest shaded region then removes $|y| > r$, to give the 4-disk that we called D .
- Finally, removing the dark regions then removes the components of sets $f^{-1}(\overset{\circ}{D}_\epsilon^2(c)) \cap \{|y| > r'\}$ where a fiber $f^{-1}(c)$ is irregular at infinity (we have also indicated the components where these fibers are regular at infinity, which are not removed).

Thus \mathbb{D} is represented by what has been left white. Recall that the parameters in this construction are chosen in the order s (sufficiently large), r' (sufficiently large), ϵ (sufficiently small), r (sufficiently large). Thus the second lightest region, which removes a neighborhood of the horizontal and finite curves of Y , is in fact much the thinnest, although we have pictured the regions all of comparable size. Most of the boundary between the dark regions and \mathbb{D} is parallel to fibers of f , with just the small parts near the intersection with the irregular fibers being transverse to fibers of f (these parts are solid tori).

In [17] it is shown that the splice diagrams at infinity are derived from the plumbing graph as above, with the parts of the splice diagram having respectively positive, zero, or negative total linking weights corresponding to respectively infinite, horizontal, or finite curves of Y . We thus see that the tori along which the splice decomposition of $\partial\mathbb{D}$ occurs are as claimed in Theorem 5.1, completing the proof (in the picture these are the places where two different grey-tones meet white). \square

We close with a comment about the minimal Seifert surface for an irregular link at infinity. We first describe how one can see such a Seifert surface in terms of the construction in the above proof.

Choose a generic line interval I from a point x of $\partial D_\epsilon^2(c)$ to a point y of $\partial D_s^2(0)$. We can assume, by choosing ϵ sufficiently small, that I does not intersect any of the ϵ -disks around irregular values except at its end point x . Then $V := f^{-1}(I) \cap \partial\mathbb{D}$ will be a Seifert surface for the link at infinity of $f^{-1}(c)$ (considered as a link in $\partial\mathbb{D}$). This V is the union of Seifert surfaces for each of the splice components described in the proof (we work with the splice decomposition before the elimination of the redundant toral annulus components):

- $f^{-1}(y)$ is a fiber of the fundamental multilink and is the compact core of a regular fiber.
- $f^{-1}(x)$ is the disjoint union of the Milnor fibers $f^{-1}(x) \cap T_i(c)$ at infinity for $f^{-1}(c)$; these are the fibers of fibered splice components corresponding to the $T_i(c)$.
- $f^{-1}(I) - \text{int}(f^{-1}\{x, y\})$ is a union of annuli giving Seifert surfaces for the Seifert fibered pieces.

Since these are minimal Seifert surfaces for these splice components, V is a minimal Seifert surface for our link at infinity (see Theorem 3.3 of [9]).

Note that the complement of the above minimal Seifert surface V in the boundary of $f^{-1}(I) \cap \mathbb{D} \cong F \times I$ is the result F_0 of removing the Milnor fibers $F_i(c)$ from $f^{-1}(x) \cap \mathbb{D}$. This $F_0 \subset \mathbb{D}$ has boundary isotopic to the link at infinity that we are considering and it realizes the minimal slice genus of this link, by the solution of the Thom Conjecture. The minimal Seifert surface V is the result of pasting doubles of the Milnor fibers at infinity onto boundary components of a copy of F_0 .

Summarizing, our link at infinity, as a link in the boundary of a 4-ball D^4 , has the property: there is a 2-manifold F containing a sub-2-manifold F_0 and an embedding $F \times [0, 1] \subset D^4$ such that $F_0 \times \{0\} \subset D^4$ is a minimal slice surface for the link while the rest of $\partial(F \times [0, 1])$ lies in ∂D^4 and is a minimal Seifert surface for the link. This is a presumably already very special property of links at infinity of affine curves, not shared by general links. Also special is the fact that $F \times \{1\} \subset \partial D^4$ and the components of $(F - \overset{\circ}{F}_0) \times \{0\}$ are the fibers of fibered splice components of the link.

REFERENCES

- [1] Artal Bartolo, E., Cassou-Noguès, P. and Dimca, A., Sur la topologie des polynomes complexes. Proceedings of Oberwolfach Singularities Conference, (1996), Brieskorn Festband, Editors: V.I.Arnold, G.-M.Greuel and J.H.M. Steenbrink.
- [2] E. Artal-Bartolo, P. Cassou-Nogués, I. Luengo Velasco, On polynomials whose fibers are reducible with no critical points, appear. *Math. Annalen* **299** (1994), 477–490.
- [3] Broughton, S. A., On the topology of polynomial hypersurfaces, *Proc. AMS Symp. Pure Math.* **40, I** (1983), 165–178.
- [4] Broughton, S. A., Milnor number and the topology of polynomial hypersurfaces, *Inv. Math.* **92** (1988), 217–241.
- [5] Dimca, A., Monodromy at infinity for polynomials in two variables, Preprint, (1998).
- [6] Dimca, A., Nemethi, Thom Sebastiani construction and monodromy of polynomials, *Prépublication* **98** (1999), Laboratoire de Math. Pures de Bordeaux C.N.R.S.
- [7] Durfee, A., Fibered knots and algebraic singularities, *Topology* **13** (1974), 47–59.
- [8] Durfee, Alan H. Five definitions of critical point at infinity. *Singularities (Oberwolfach, 1996)*, *Progr. Math.*, **162**, 345–360
- [9] Eisenbud, D. and Neumann, W.D., *Three-dimensional link theory and invariants of plane curve singularities*. *Ann. Math. Stud.* **110**, Princeton. Princeton Univ. Press (1985).
- [10] Hirsch, M. *Differential Topology*, Graduate Texts in Math. **33** (Springer Verlag, 1976).
- [11] M. Jankins and W.D. Neumann, Lectures on Seifert manifolds, *Brandeis Course Notes* **2** (1983).
- [12] Lamotke, Klaus, Die Homologie isolierter Singularitäten. *Math. Z.* **143** (1975), 27–44.
- [13] Milnor, J., *Singular points of complex hypersurfaces*, *Ann. Math. Stud.* **101**, Princeton University Press, (1968).
- [14] Némethi, A., Zaharia, A., On the bifurcation set of a polynomial and Newton boundary, *Publ. RIMS* **26** (1990), 681–689.
- [15] Neumann, W.D., Splicing algebraic links, in *Complex Analytic Singularities*, Advanced Studies in Pure Math. **8** (1986), 349–361.
- [16] Neumann, W.D., Complex algebraic curves via their links at infinity, *Invent. Math.* **3**, (1989), 445–489.

- [17] Neumann, W.D., Irregular links at infinity of complex affine plane curves, Quarterly J. Math. (to appear).
- [18] Neumann, W.D. and Norbury, P., Monodromy and vanishing cycles of complex polynomials, Duke Math. J. (to appear).
- [19] Neumann, W. and Rudolph, L. Unfoldings in knot theory, Math. Ann. **278**, (1987), 409-439. *Corrigendum*, Math. Ann. **282**, (1988), 349-351.
- [20] Parusiński, A. On the bifurcation set of a complex polynomial with isolated singularities at infinity, Compositio Math. **97** (1995), 369–384.
- [21] Parusiński, A. A note on singularities at infinity of complex polynomials, *Simplectic singularities and geometry of gauge fields*, Banach Center Publ. **39** (1997), 131–141.
- [22] Pham, F., Vanishing homologies and the n variable saddlepoint method, AMS Proc. Sympos. Pure Math. **40,II** (1983), 319–333.
- [23] Siersma, D., Tibăr, M. Singularities at infinity and their vanishing cycles, Duke Math. J. **80** (1995), 771–783.
- [24] Suzuki, M. Propriétés topologiques des polynômes de deux variables complexes et automorphismes algébriques de l'espace C^2 , J. Math. Soc. Japan **26**, (1974), 241–257.
- [25] Masakazu Suzuki, Sur les opérations holomorphes du groupe additif complexe sur l'espace de deux variables complexes. (French) Ann. Sci. École Norm. Sup. (4) **10** (1977), 517–546.
- [26] Tibăr, M., On the monodromy fibration of polynomial functions with singularities at infinity, C. R. Acad. Sci. Paris, **324**, Série I (1997), 1031–1035.
- [27] Tibăr, M., Regularity at infinity of real and complex polynomial functions, *Singularity Theory, C.T.C. Wall Anniversary Volume*, (Cambridge U. Press).

DEPARTMENT OF MATHEMATICS AND STATISTICS, THE UNIVERSITY OF MELBOURNE,
VIC 3010, AUSTRALIA

E-mail address: `neumann@ms.unimelb.edu.au`

DEPARTMENT OF MATHEMATICS AND STATISTICS, THE UNIVERSITY OF MELBOURNE,
VIC 3010, AUSTRALIA

E-mail address: `norbs@ms.unimelb.edu.au`